ceramics

Article

Islamic Middle Ages Pottery from Muge (Portugal), Serradinho Archaeological Site—A Long-Lasting Tradition of Pottery Production

Carlos Andrés Camara [1], Gonçalo Lopes [2], Nicola Schiavon [1], José Mirão [1] and Massimo Beltrame [1,*]

[1] Hercules Laboratory, University of Evora, Palacio do Vimioso, Largo Marquês de Marialva 8, 7000-809 Evora, Portugal; ccamarav@gmail.com (C.A.C.); schiavon@uevora.pt (N.S.); jmirao@uevora.pt (J.M.)

[2] Tawn Hall of Montemor O-Novo, Largo dos Paços do Concelho 5, 7050-169 Montemor-o-Novo, Portugal; g.simoeslopes@gmail.com

* Correspondence: massimo@uevora.pt

Abstract: During the Islamic period, ceramic workshops were commonly established in settlements throughout the *Gharb al-Andalus* region (Western Iberia at the time), to produce ceramics for local supply. Along the middle valley of the Tagus river (i.e., nowadays central Portugal), hundreds of Islamic ceramic sherds, either glazed or common wares, were recovered over different archaeological excavations. At the archaeological site of Serradinho, located at Muge (Municipality of Salvaterra de Magos, Santarem District, Portugal), a fortuitous finding was unearthed during agricultural works in which ceramic sherds from the Emiral (8–9th century) to the Almoravid (mid–12th century) period were recorded. The uninterrupted time lapse evidenced by these ceramic artefacts is a one-off opportunity to trace back early Islamic ceramic production and to link it with the long-lasting ceramic tradition documented at Muge by ethnographic studies. In this study, insights into the provenance of raw materials and the pottery-manufacturing processes will be approached by means of different optical and analytical methods, namely Optical Microscopy (OM), X-Ray Diffraction (XRD), X-Ray Fluorescence (XRF), Scanning Electron Microscope, Energy Dispersive X-ray Spectroscopy (SEM-EDS) and granulometric tests on sediments offering some interesting parallels between archaeological and modern ceramic production. Results suggested that most ceramics were locally produced, while others were imported into the settlement during the Islamic Middle Ages. Moreover, data indicate that a locally available raw material which is still used nowadays for the production of traditional ceramics had been employed. This result confirms the exploitation of the same raw material over time, linking Islamic Middle Ages ceramic production to the modern one.

Keywords: Islamic workshops; Gharb al-Andalus; Serradinho; ceramic production; raw materials; traditional ceramics.

Academic Editor: Gilbert Fantozzi

Received: 28 February 2025
Revised: 20 March 2025
Accepted: 24 March 2025
Published: 27 March 2025

Citation: Camara, C.A.; Lopes, G.; Schiavon, N.; Mirão, J.; Beltrame, M. Islamic Middle Ages Pottery from Muge (Portugal), Serradinho Archaeological Site—A Long-Lasting Tradition of Pottery Production. *Ceramics* **2025**, *8*, 31. https://doi.org/10.3390/ceramics8020031

1. Introduction

The conquest of the Iberian Peninsula by Berber armies started in 711 AD, and it was almost concluded in 714 AD. The city of Santarem (Figure 1) peacefully surrendered in the same year, and most of the Iberian Peninsula became an emirate of the Umayyad Caliphate of Damascus. In the early 8th century, the city became a *Kura*, one of the territorial demarcations into which *al-Andalus*, the ancient Islamic Iberian Peninsula, of the province of Merida until the end of the Caliphate of Cordoba (early 11th century). Over this time span, the Kura of Santarém (*Shantarin*—Islamic name) would be important for the Muslim administration of the *Gharb al-Andalus* (i.e., Western Iberia during the Islamic time) due to its closeness to the Tagus river which, in turn, would endow this border zone (Marca) with a strategic, economic/commercial position highly sought after since the beginning of the Portuguese Reconquista [1].

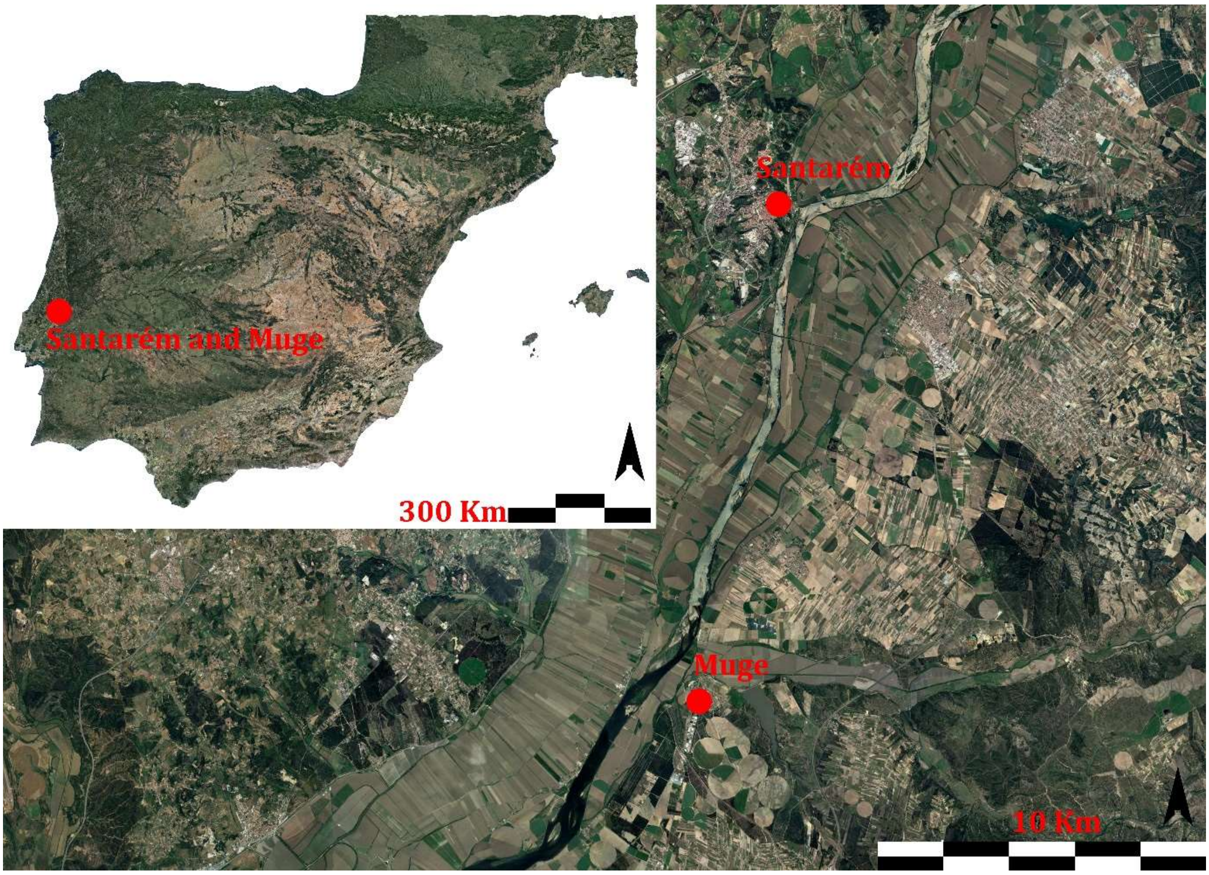

Figure 1. Identification of Santarem and Muge along the middle Tagus Valley in the Iberian Peninsula. Adapted using images collected with Google Earth Pro.

After the Arab conquest of the *al-Andalus* (i.e., Iberian Peninsula during the Islamic Middle Ages), the Islamic administration structured the area following the old Roman political-administrative division, with the *Kura* of Santarém controlling a vast area in the middle of the Tagus valley [1,2]. Arab sources generally neglected or omitted the description of rural communities (qarya/qurul), focusing on the main Islamic cities (madina/mudun) or regions (kuwar/kura) across the *Gharb al-Andalus*. In this sense, the concept of the rural space is rather vague in documents, except for a mention by *Dikr bilad al-Andalus* of "more than a thousand villages" [3] (p. 58) across the *Kura* of *Shantarin*, which reveals the dense population that once inhabited the middle Tagus valley [2,4].

The proximity of Santarém to the Tagus river would be economically exploited over the first centuries of the Islamic domination (8th and 12th centuries), turning the city into an important peripheral town across the al-Andalus with demographically strong, productive peri-urban settlements scattered in a non-homogeneous pattern close to irrigable plains and/or fortresses [1,2,5–7]. For instance, the Islamic settlement of Muge (Figure 1), located at Muge (i.e., 10/15 km downstream from Santarém), represents one of the several small settlements located along a watercourse and over an elevated plain where its cultivated areas would exploit the fertile lands and river flooding episodes [2,7,8]. Following several periods of political instability between the 10th and the end of the 11th centuries, by the end of the 11th century, the *al-Andalus* was included in the Almoravid Kingdom (i.e., a

Berber dynasty from Morocco). In the middle of the 12th century, the whole Tagus valley was included in the Portuguese kingdom, despite the effort by another Berber dynasty, the Almohad, to take back the former Tagus valley borders in the same century [1,9].

After the inclusion of the Tagus valley in the Portuguese kingdom, the territory became densely occupied by a population marked by strong ethnic and cultural diversity (e.g., Christians, Mozarabs, Muladi, Arabs and Berbers) [4], with the Portuguese rulers fostering the colonisation of the newly conquered lands by offering royal statutes (forais) to villages and communities, bestowing on them autonomy and regulation. The Christian sources documented the first initiatives leading to the occupation, space ordering and local authority structure in 1159, following the forais of Lisbon and Santarem in 1179 [1,2,6,9]. Under these political circumstances, Muge would thrive over time, resisting the reconquest struggles and changing from a former Islamic settlement to a recognised village by the end of the Middle Ages [8].

The settlement of Muge was established on former Islamic remnants and consisted of a typical Medieval farm characterised by a surrounding land domain, a central house or houses along with barns and other facilities for property service linked to an agriculturally based economy [8,10]. Although agriculture was the main activity, the territory was extremely rich in natural resources such as clay [7,9], favouring the domestic and industrial production of ceramic artefacts [5,11]. Post-reconquest Christian records have documented the presence of domestic and industrial kilns either in urban or rural centres, for the making of bread, tiles, lime, bricks and vessels [5,12].

By the beginning of the 20th century, a local traditional ceramic production at Muge and its compositional characterisation is reported by Charles Lepierre [13], a study that was-completed froman ethnographic perspective by Joaquin do Santos Junior [14]. Nowadays, few traditional ceramic workshops are still active, but these traditional economic activities are extremely valuable [11]. In addition, ancient production methods are still employed today, with the locally available raw material preferred to the industrial one. The best example is represented by the workshop of the ceramist Domingos Gomes da Silva in Muge. His workshop supplies an ever-smaller local market, and he has been a reference throughout Portugal for keeping an ancestral ceramic knowledge over time, preserving the memory of an ethnographically documented cultural tradition for future generations [11,15]. This includes all steps involved in traditional ceramic production, from raw material selection to final ceramic finishing stages. Within this framework, the possibility ofusing the ancestral knowledge of a traditional ceramist might shed new light into to the Islamic Middle Ages of the area. Furthermore, it would enable not only to explore Islamic ceramic technology at Muge but also to evaluate the exploitation of either similar or same raw materials for ceramic production. Moreover, it will also help in assessinglocal economy processes (i.e., rural) and compare them with the ones operatingin main administrative Islamic centre during the Middle Ages (i.e., Santarém), where the local production of different Islamic ceramic wares has already been assessed [16,17]. These objectives will be achieved thanks to the archaeometric analysis of fifteen Middle Ages Islamic ceramic samples recovered during a archaeological intervention around Muge in 1995, leading to the discovery of the Serradinho archaeological site. Ceramics will also be compared with locally available raw materials still employed by local ceramists for the production of traditional ceramics.

2. Geological Setting

The Tagus valley (Figure 2) is a natural depression that belongs to the Lower Tagus Cenozoic Basin (LTCB), following a NNE/SSW axis (north-north east/south-south west) in the southwestern region of the Iberian Peninsula [18]. This basin was fully covered by different sedimentary deposits during the Miocene (MP, M4, M5) and Pliocene (P1, P2), mainly shaping the right bank of the river [19]. During the same geological periods, the sedimentary conditions changed, favouring the deposition of lacustrine limestone layers in the upper Miocene and Pliocene deposits [20]. Pleistocene fluvial terraces (Q, Q1, Q2, Q3, Q4) and modern deposits (A, a, Ad, As) came afterwards, composing the alluvial plains on the left side of the Tagus river [21,22]. In this area, at 70–75 km northeast of Lisbon lays the small village of Muge characterized by a geological setting that is rather homogeneous, which consists of modern flood deposits (a), superficial sands (As) and Pleistocene fluvial terraces (Q2–Q3) outcropping at roughly 4–5 km from the village (see legend in Figure 2). In the surrounding areas, some Miocene deposits of clay (MP) also outcrop [23].

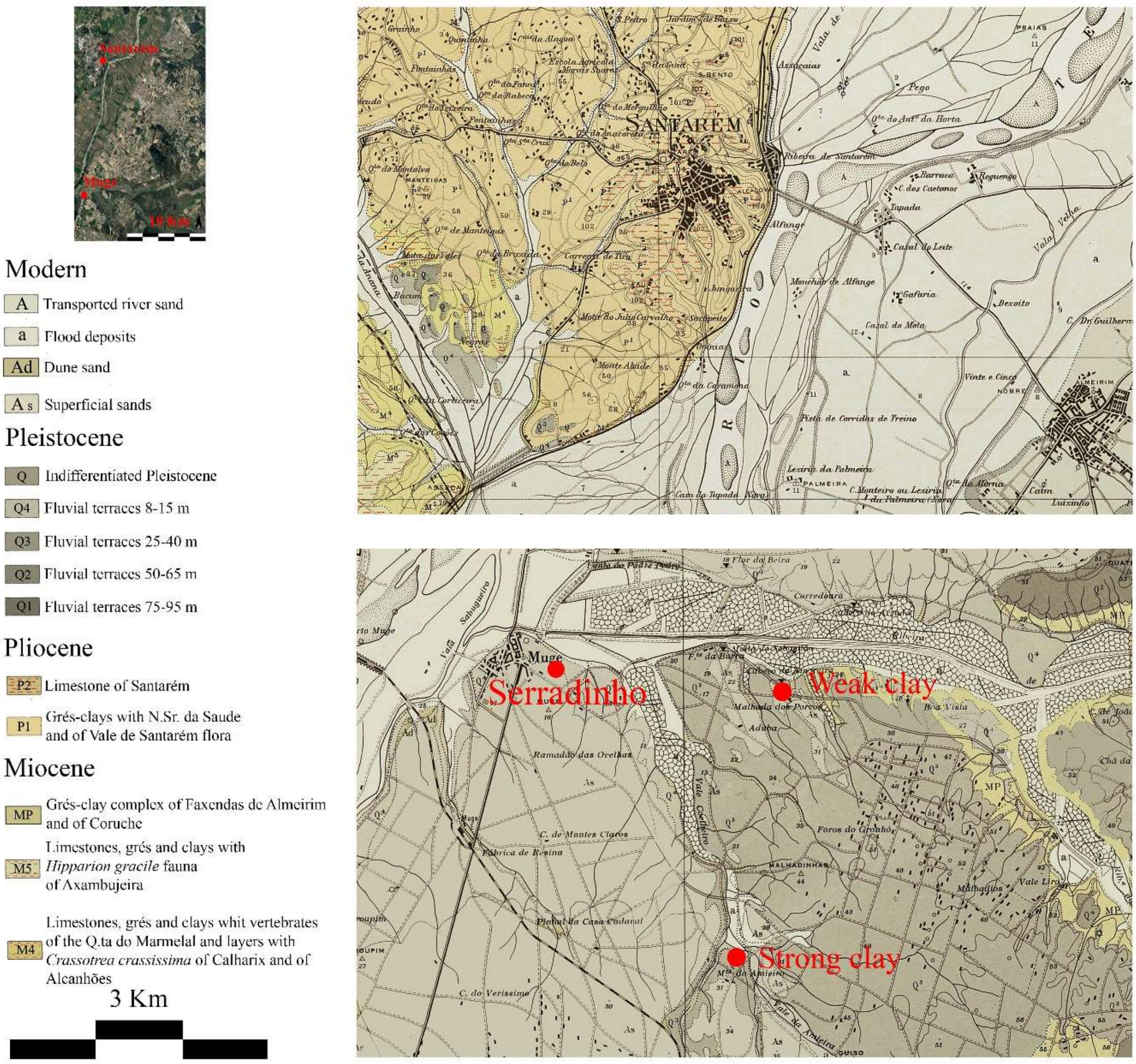

Figure 2. Excerpt from the geological map of Portugal scale 1:50,000 elaborated with information from [21] Zbyszewski, Serviços Geológicos de Portugal, 1953 and from [22] Zbyszewski and Da Viega, Serviços Geológicos de Portugal, 1968.

3. Materials and Methods

3.1. Archaeological Ceramic Retrieval Context and Analysed Samples

The archaeological finding happened in 1995 during agrarian works that involved the superficial removal of soils for the plantation of vineyards across a space known as Serradinho, at the "*Quinta de Santo Antonio or Horta da Casa Cadaval*". This area, owned by a firm related to the Duke of Cadaval, belongs to the village of Muge (Municipality of

Salvaterra de Magos, District of Santarém) and is located over a small, elevated platform at 100 metres east (Figure 2) from the current administrative boundaries of the urban area [8].

The ceramic sherds recovered from the Serradinho archaeological site originally amount to fifty objects which were typologically characterized in order to define their relative chronologies throughout the Islamic ceramic production. Most of the ceramic samples can be defined as "common ceramic ware" for domestic use, with a red-orange ceramic paste, probably fired under oxidising conditions, with the exception of five light-coloured ceramic paste fragments with red-painted decorations, green and brown glazed decorations and with total *cuerda seca* glazed decorations. The typological study has already been published by Gonçalo Lopes [8] and, based on typology and decoration characteristics, the ceramic pieces can be chronologically placed between the Emiral and the Almoravid periods (from 9th to mid-12th centuries). Thus, the existence of a former Islamic village and the possibility of a local ceramic production were confirmed. In the present study, fifteen pieces (Table 1, Figures 3 and 4) from the whole ceramic assemblage were considered. The decision to select just 15 out of 50 samples for scientific analyses was taken in collaboration with the legal owner of the ceramic assemblage for two main reasons Firstly, the macroscopic observation of the ceramic samples suggested that the "common ware ceramic group" was highly represented and typologically similar, so to perform archaeometric analysis of the whole assemblage was not economically justified. Secondly, Muge ceramics represent the only archaeological evidence of the Middle Ages Islamic presence within the territory of the municipality, and it was important to preserve ceramic fragments for displaying at the inauguration of the local Museu do Concelho, organised by the Municipality of Salvaterra de Magos, which took place on 8 September 2024.

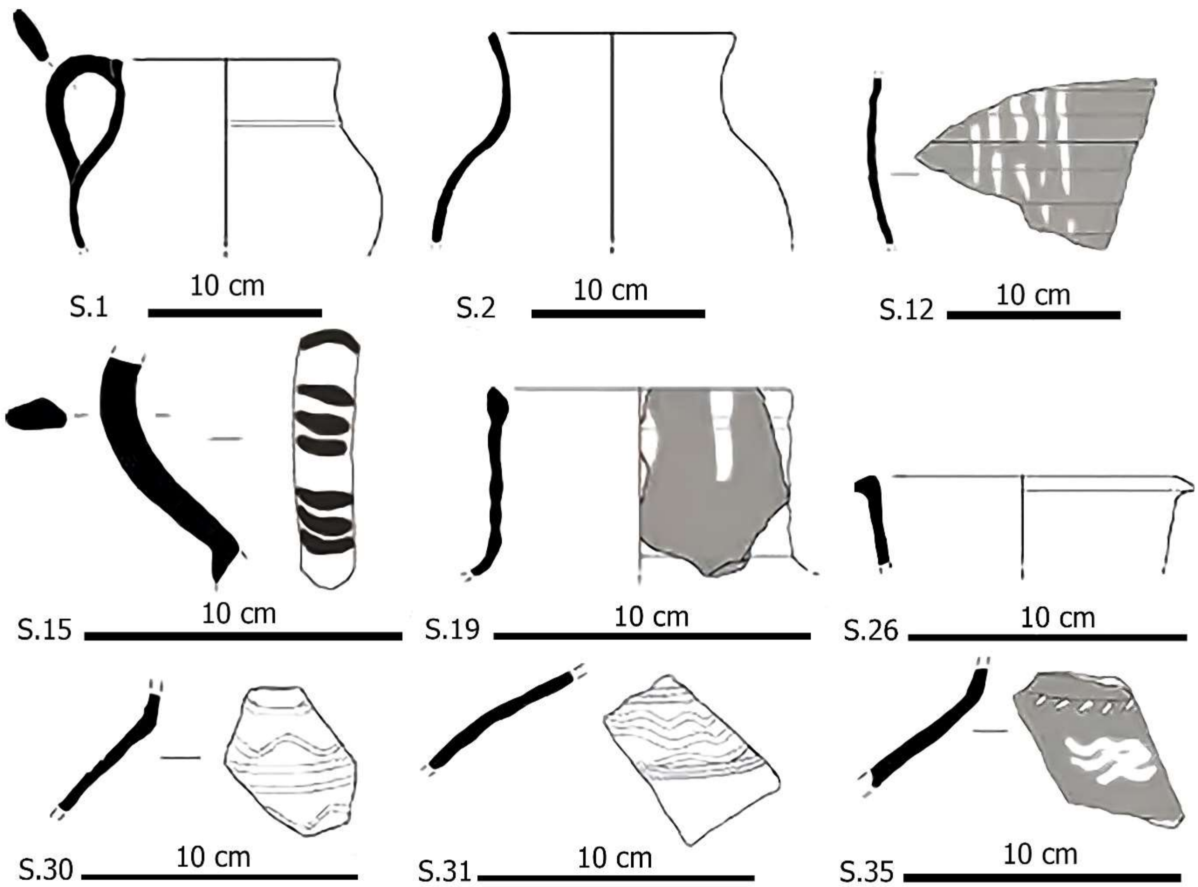

Figure 3. Ceramic samples considered in this study.

Table 1. List of analysed ceramic pieces.

Reference	General Classification	Typology	Function	Decoration	Century	Period	Ref. in [8] Lopes
Sample 1	Common ware	Cooking pot “Panela”	Fire ceramic	None	9–10th	Emiral?	Drawing 1—Figure 6 (p. 177)
Sample 2	Common ware	Cooking pot “Panela”	Fire ceramic	None	9–12th	Taifa/Almoravid	Drawing 2—Figure 6 (p. 177)
Sample 12	Common ware	Cooking pot “Panela”	Fire ceramic	White painted	11–12th	Taifa/Almoravid	Drawing 12—Figure 6 (p. 177)
Sample 15	Light coloured	Little jar	Liquid container	Red painted	11th	Taifa	Drawing 15—Figure 8 (p. 179)
Sample 19	Common ware	Little jar	Liquid container	White painted	11–12th	Taifa/Almoravid	Drawing 19—Figure 8 (p. 179)
Sample 26	Common ware	Big jar	Liquid container	None	10–11th?	Caliphal/Taifa?	Drawing 26—Figure 9 (p. 179)
Sample 30	Common ware	Big jar	Liquid container	Incisions	11–12th?	Taifa/Almoravid?	Drawing 30—Figure 9 (p. 179)
Sample 31	Common ware	Big jar	Liquid container	Incisions	11–12th?	Taifa/Almoravid?	Drawing 31—Figure 9 (p. 179)
Sample 35	Common ware	Big jar	Liquid container	White painted	12th	Almoravid	Drawing 35—Figure 9 (p. 179)
Sample 37	Common ware	Big jar	Liquid container	White painted	12th	Almoravid	Drawing 37—Figure 9 (p. 179)
Sample 39	Common ware	Cooking pot “Caçoilas e/o Tijelas”	Fire ceramic	None	10–12th	Caliphal/Taifa	Drawing 39—Figure 10 (p. 180)
Sample 41	Common ware	Cooking pot “Caçoilas e/o Tijelas”	Fire ceramic	White painted	11–12th	Taifa/Almoravid	Drawing 41—Figure 10 (p. 180)
Sample 44	Common ware	Big earthen pot	Storage ceramic	Moulded plastic decoration	10–11th	Caliphal/Taifa	Drawing 44—Figure 12 (p. 181)
Sample 48	Light- coloured	Bowl	Table ware	Red painted	10–11th	Caliphal/Taifa	Drawing 48—Figure 15 (p. 183)
Sample 50	Light- coloured	Bowl	Table ware	*Cuerda seca*	12th	Almoravid	Drawing 50—Figure 17 (p. 183)

3.2. Sediment Sampling

Two different raw materials were also sampled in the vicinity of the archaeological site and the village of Muge (Figure 2). Raw materials were identified in the geological layer Q3, which correspond to fluvial sedimentary terraces. These raw materials were named by local ceramists “strong/fat” and “weak/light” clays (Figure 5), and ceramists used to mix them based on the intended function of the object. The “strong clay” is generally more plastic and stickier when water is added, while the “weak clay” is enriched in inclusions when compared to the previous one.

3.3. Methods

The archaeometric study of the ceramic samples included OM, powder XRD, XRF, and SEM-EDS. OM was performed after the preparation of thin sections using a Leica DM-2500-P optical microscope coupled with a Leica MC-170-HD camera (Leicamicrosystems, Wetzlar, Germany). Minerals and rock fragments were identified. In addition, characteristics concerning ceramic paste (homogeneity, optical activity, colours), porosity (shape), and temper (sorting, spacing, abundance, granulometric distribution) were described [24]. Temper size and roundness were evaluated according to the Udden–Wentworth scale [25,26].

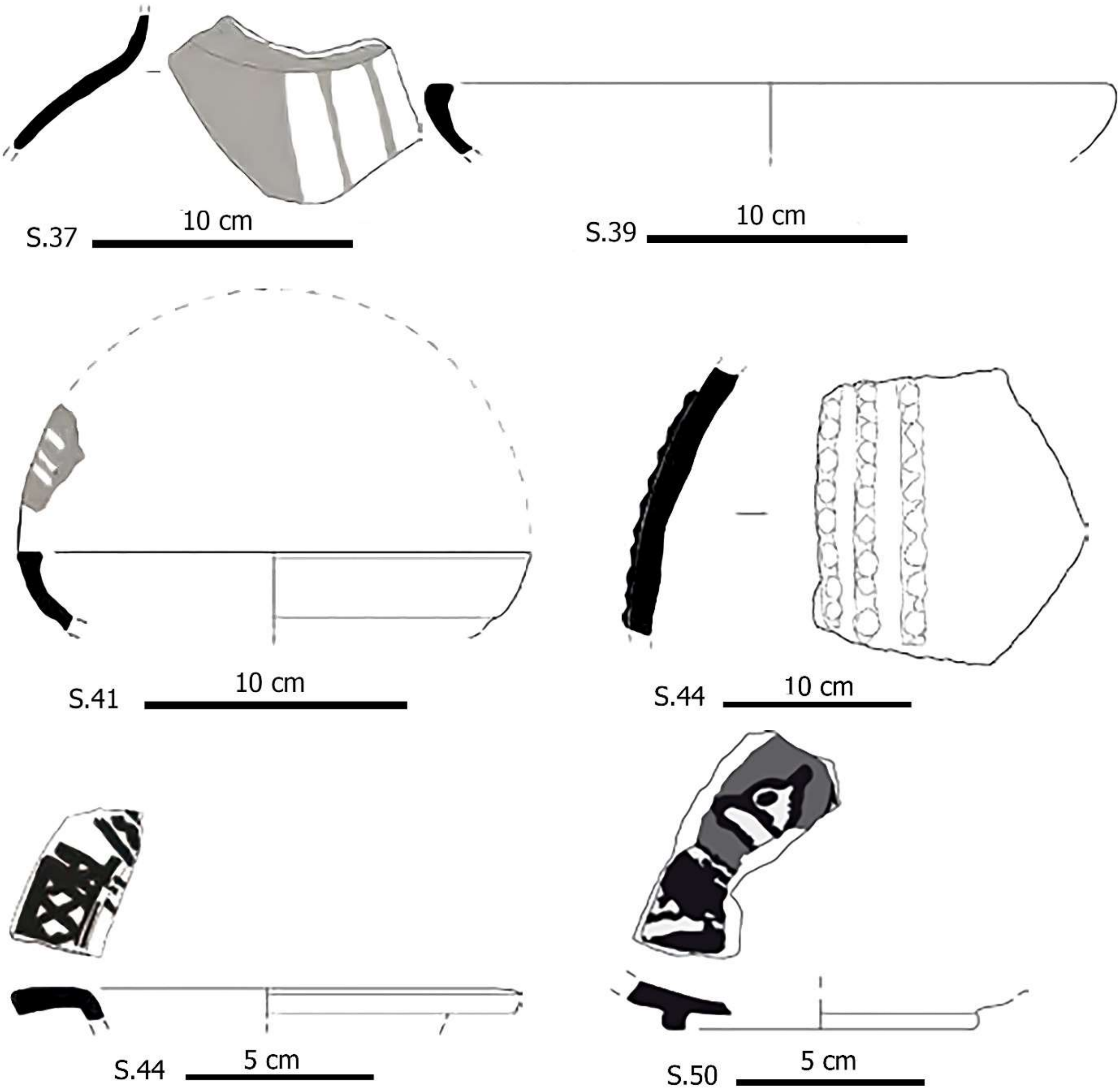

Figure 4. Ceramic samples included in this study.

Bulk mineralogy by powder XRD was determined using a Bruker D8 Discover diffractometer (Bruker, Karlsruhe, Germany) equipped with a copper X-ray radiation source. The working conditions were as follows: X-ray tube was operated at 40 kV and 40 mA, step size at 0.05°/2θ, measuring time equal to 1s/step and collection of patterns from 2° to 75°2θ. The Diffract-EVA software (Release 2019) and the PDF-2 mineralogical database (International Center for Diffraction Data—ICDD) were employed to interpret results. Semi-quantitative results and reference intensity ratio (RIR) analyses [27] are presented for all ceramic samples.

Chemical composition of samples, including major oxides and some trace elements, was determined using a Bruker S2 Puma (Bruker, Karlsruhe, Germany) energy-dispersive XRF spectrometer (ED-XRF), equipped with a silver X-ray tube, and calibrated by 36 standard reference materials. The specimens were fused glass beads made up of a 1:10 sample/flux ratio. Results included oxides/elements concentrations and associated instrumental statistical errors. Software used for data acquisition and processing was Spectra Elements 2.0. Loss on ignition (LOI) was evaluated by calcination using roughly 1 g of sample material [28].

Figure 5. Raw materials collected in the vicinity of the archaeological site and the village of Muge. Pictures (**A**,**C**) represent the "strong" clay, while pictures (**B**,**D**) represent the "weak" clay.

The glazed decoration of sample 50 was also characterised from the microstructural/chemical point of view. The whole examination was performed by using a variable pressure Hitachi S-3700N scanning electron microscope (Hitachi, Krefeld, Germany), whose microanalysis system comprised of a Bruker XFlash 5010 X-ray energy drift detector (Bruker, Karlsruhe, Germany) with a spectral resolution of 129 eV (FWHM/Mn Kα). The working conditions were the following: acceleration voltage at 20 kV, 120 μA and a pressure at 40 Pa inside the chamber of analysis. Standardless PB/ZAF quantitative analyses were acquired utilising Bruker ESPIRIT software (Version 3.2-42.0–32 bit). Detection limits for major oxides (>Na_2O) were in the order of 0.1 wt% [29].

Sampled clays were analysed in the following way: about 0.5 kg of each clay was disaggregated in a porcelain mortar and sieved through 2, 1, 0.5, 0.25, 0.125 and 0.063 mm sieves to obtain the grainsize distribution. Retained fractions were weighted and described using the Udden–Wentworth scale [25]. Afterwards, different batches of 0.5 kg of both raw materials were divided into 5 different parts to evaluate how sieving influenced raw material samples mineralogy and chemical composition. The untreated raw material and fractions smaller than 0.5, 0.25, 0.125 and 0.063 mm were isolated and analyzed by XRD and XRF using the same methodology adopted for archaeological ceramics.

4. Results and Discussion

4.1. Archaeological Ceramics

4.1.1. Optical Microscopy (OM)

OM Results Identified Three Different Ceramic Fabrics

Fabric 1 (Figure 6a). A total of twelve different ceramic samples pertain to fabric 1, including ceramic wares with different functions, such as cooking pots, small/big jars and the big earthen pot. Samples were undecorated, painted white, or with incisions or with moulded plastic decorations. The ceramic paste is generally brown/red in colour, slightly homogeneous, optically active and showing nonhomogeneous clay pellet inclusions. Temper concentration varies between the 10% and 20%, and grain shape varies between angular and sub-rounded. Grain size varies between very coarse sand and coarse silt, alignment is weak/moderate, sorting is poor, and grain size distribution is bimodal. Porosity is high mainly consisting of vesicles (up to 50–60 µm) and elongated planar voids (between 300–1000 µm). Quartz, muscovite, potassium rich feldspar, sodium rich plagioclase and tourmaline were mainly identified. Amongst rock fragments, quartzite, sandstone, and granitic rock fragments were observed.

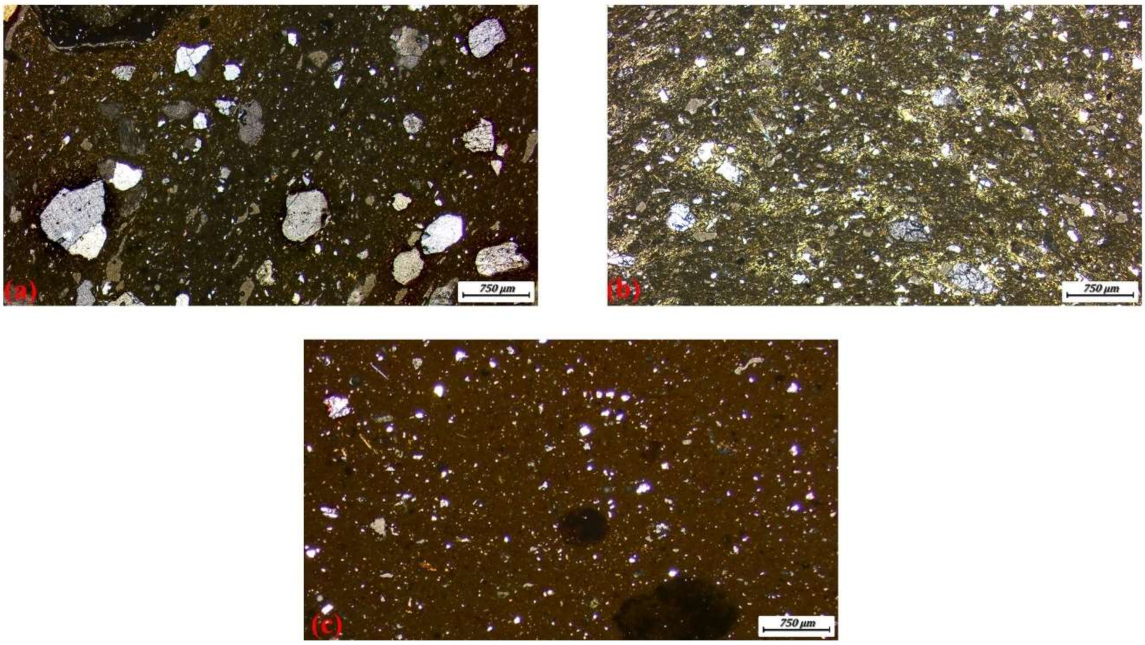

Figure 6. Picture of representative samples of fabric 1 (sample 12, (**a**)), fabric 2 (sample 48, (**b**)) and fabric 3 (sample 50, (**c**)), collected in XPL mode at 25× magnification.

Fabric 2 (Figure 6b). In total, two ceramic samples pertain to fabric 2, including one bowl and one little jar with red-painted decorations (Samples 15 and 48). The ceramic paste is generally light brown, moderately homogeneous, and unhomogeneous clay pellets are rare. Temper concentration varies between the 5% and 10%. Temper grain morphologies vary between sub-angular and rounded, but rounded grains are clearly more abundant. Grain size varies between coarse sand and coarse silt, grain size distribution is unimodal, with alignment and sorting moderate. Porosity is clearly lower when compared to fabric 1, and it is mainly characterised by vesicles (roughly 50 µm in size) and by a minor amount of elongated planar voids (between 200 and 500 µm). Quartz, muscovite, potassium rich feldspar, sodium rich plagioclase and tourmaline were mainly identified. Amongst rock fragments, quartzite and rare granitic rock fragments were observed.

Fabric 3 (Figure 6c). Fabric 3 only includes sample 50, which is a bowl with total *cuerda seca* glazed decorations. The ceramic paste is red-buffy in colour (suggesting high calcium content in the ceramic matrix), moderately homogeneous and with rare non homogeneous clay pellets. Small lime rich nodules were also observed. Temper concentration is low (roughly 5%), and temper morphology varies between sub-angular and sub-rounded. Grain size varies between coarse sand and coarse silt, grain size distribution is unimodal, alignment is moderate, and temper is well sorted. Porosity is just composed by vesicles up to 50–60 µm in diameter. Quartz, muscovite (quite abundant), potassium rich feldspar, rare plagioclase and rare amphibole were mainly identified. Amongst rock fragments, just greywacke fragments (i.e., rare) were detected.

From a technological point of view, data collected during OM observations suggested that three different fabrics were employed for the production of different ceramic wares. More specifically, it is the decoration technique applied that represents an important variable. Fabric 1 was just employed to produce undecorated, white-painted, and with incised/plastic decoration ceramics. Fabric 2 was just employed to produce red-painted ceramics, and fabric 3 was employed to produce the total *cuerda seca* glazed ceramic sample. These observations suggest the use of three different raw materials in pottery production. Typology does not seem to represent an important variable. In the case of fabric 1, different ceramic wares were produced, as well as in the case of fabric 2. Only one sample has been included in fabric 3, and, therefore, it is not possible to speculate about the correlation between typology and raw material selection. From a chronological perspective, we can generally assume a continuity in raw material exploitation, with the exception of fabric 3 for the same reasons mentioned above. Regarding ceramic provenance, as minerals and rock fragments identified are compatible with the local geology, most likely, fabric 1 and fabric 2 were probably locally and/or regionally produced. Also, the presence of rounded grains suggests "transportation" and consequently the exploitation of a raw material probably collected close to a river/stream. Similar results were obtained during the analysis of Islamic Middle Ages ceramics at Santarém [16,17], which were produced using locally available raw materials close to the city.

4.1.2. Powder X-Ray Diffraction Results of Ceramic Samples—P-XRD

XRD results identified two different mineralogical groups (see XRD group—Table 2), and ceramic fragments included in different fabrics could be considered within the same XRD group. The only sample that was included in XRD group 2 is sample number 50, the one with total *cuerda seca* glazed decoration. Generally, results corroborate OM observations.

In XRD group 1, samples of fabric 1 and 2 are included. The bulk mineralogy is very similar, and it mainly includes quartz, illite/muscovite, hematite, feldspars, and rutile. The identified mineralogical species support OM observations.

On XRD group 2, only the sample number 50 from fabric 3 is included. Quartz, illite/muscovite and feldspars as well as amphibole were identified. In addition, calcium/magnesium rich mineralogical phases such as inosilicate (i.e., pyroxene—diopside) and sorosilicate (i.e., akermanite) were also observed along with an abundant concentration of plagioclases (i.e., probably calcium rich). Considering that these mineralogical phases were not observed during OM observation, with the exception of some plagioclase crystals, they surely developed inside the ceramic paste due to the suggested firing temperature reached in the kiln during the firing process. Thus, XRD analyses underlined two different and linked aspects of ceramic technologies, namely raw material selection, characteristics and ceramic thermal history.

Table 2. Semi-quantitative XRD results of archaeological ceramics expressed in percentage (%). Q, quartz; H, hematite; Py, pyroxene; Kf, potassium-rich feldspar, Na-Pl, Na-rich plagioclase; Ca-Pl, Ca-rich plagioclase; Ill/Mus, illite/muscovite; Ak, akermanite; Rut, rutile; Amp, amphibole.

ICDD Reference Code			01-080-0743	01-072-0469	01-075-1092	01-076-0831	00-009-0469	00-041-1486	01-080-0743	01-087-0049	01-075-1756	01-085-2157
Sample	**Fabric**	**XRD Group**	**Q**	**H**	**Py**	**Kf**	**Na-Pl**	**Ca-Pl**	**Ill/Mus**	**Ak**	**Rut**	**Amp**
Sample 1	1	1	60	1		23	4		11			
Sample 2	1	1	55	6		27	3		13		1	
Sample 12	1	1	57	1		20	3		19		1	
Sample 15	2	1	57	1		22	2		17		1	
Sample 19	1	1	61	1		20	6		12		1	
Sample 26	1	1	50	1		32	3		14		1	
Sample 30	1	1	59	1		23	3		15			
Sample 31	1	1	61	1		21	2		15			
Sample 35	1	1	63	1		18	5		12		1	
Sample 37	1	1	66	1		21	2		11			
Sample 39	1	1	57	1		22	4		16			
Sample 41	1	1	57	1		18	6		18			
Sample 44	1	1	60	1		23	5		10		1	
Sample 48	2	1	63	1		21	2		13			
Sample 50	3	2	31		20	7		25	10	2		3

The development of specific mineralogical phases during firing indicates the selection of two different raw materials [30–35]. In the case of XRD group 1, the raw material selected can be defined as "calcium poor". Moreover, calcium-rich high-temperature mineralogical phases did not develop. Conversely, this happened in the case of XRD group 2, indicating that the raw material selected was "calcium rich". This is a specific technological choice generally adopted in the production of Middle Ages glazed ceramics both in the Iberian Peninsula and the Middle East to facilitate the application of glazed decorations to ceramic bodies [23,36–38]. Considering XRD group 1, the presence of two different mineralogical phases, hematite and illite/muscovite, is diagnostic. Hematite generally develops at 750 °C within the ceramic paste of a calcium-poor raw material [31,34], while illite/muscovite crystalline structures normally collapse above 950 °C [32,34]. Thus, XRD group 1 ceramics were fired between 750 °C and 950 °C. In the case of sample number 50, XRD group 2, diopside, akermanite and calcium-rich plagioclase are the diagnostic mineralogical phases to evaluate thermal history. Inside calcium-rich raw materials, calcite is an important mineralogical phase, and it normally disappears above 750 °C [31,33,39]. Illite/muscovite, as mentioned before, disappears above 950 °C. Hematite does not form because free iron is incorporated inside a diopside crystalline structure at temperatures in the 750–800 °C range, while akermanite forms in the range between 950 °C and 1100 °C [33,39]. Above 1100 °C, akermanite decomposes, and calcium-rich plagioclase starts to nucleate. So, it is possible to state that sample number 50 was probably fired in a temperature range between 950 °C and 1100 °C [34].

4.1.3. X-Ray Fluorescence Results of Ceramic Samples—XRF

The complete XRF dataset can be found in a separate Supplementary Materials file, attached to this article. Chemical analyses of samples by XRF spectroscopy corroborated OM and XRD results. Samples included in fabric 1 have an Fe_2O_3-rich ceramic paste, fabric 2 is poor in Fe_2O_3 and enriched in Al_2O_3, while the only sample included in fabric 3 is enriched in CaO and Sr and depleted in Al_2O_3 and SiO_2. These results suggest the exploitation of three different raw materials for ceramic production. In the case of fabric 1 and 2, a similar technology for production was already reported in the city of Santarém, located 15–20 km upstream from the village of Muge [17].

4.1.4. SEM-EDS of the Glazed Decoration (Sample 50)

The micro-structural and chemical characterisation of the glazed decoration of the sample number 50 (Tables 1 and 3, Figures 4 and 7) was performed in order to evaluate the glaze technology used, the application technique and the chromophore elements employed to obtain different coloured glazes. The fragment shows a total *cuerda seca* polychromatic glazed decoration (i.e., in white, green and black) on the inner side of the bowl and a honey glaze on the outer surface. The *cuerda seca* technique is characterised by a design/composition (i.e., the *cuerda*) generally obtained on a pre-fired ceramic body using a mixture of different manganese and/or iron oxides [1,40,41]. Afterwards, the decoration was completed using a different coloured preparation [42], completely or partially covering the surface of the piece with a glazed decoration (i.e., total vs. partial *cuerda seca* decoration).

Table 3. SEM-EDS data, thickness and major oxides concentration of coloured glazes decorations.

Glaze Colour	Position	Thickness (μm)	Na_2O	MgO	Al_2O_3	SiO_2	PbO	K_2O	SnO_2	CaO	TiO_2	MnO	Fe_2O_3	CuO	SiO_2/PbO	Na_2O+ K_2O
White glaze	Inner side	130	1.43	0.34	2.36	36.53	52.34	1.46	1.44	2.90			1.20		0.7	2.89
Black glaze	Inner side	110	1.39	0.33	1.30	36.41	48.92	1.33	3.56	2.84		2.76	1.16		0.74	2.74
Green glaze	Inner side	160	0.44	0.29	2.36	28.38	55.96	1.61	2.49	4.31	0.48		1.93	1.75	0.51	2.05
Honey glaze	Outer side	90	1.02	0.49	5.18	34.43	51.63	1.51		3.60	0.21		1.93		0.67	2.53

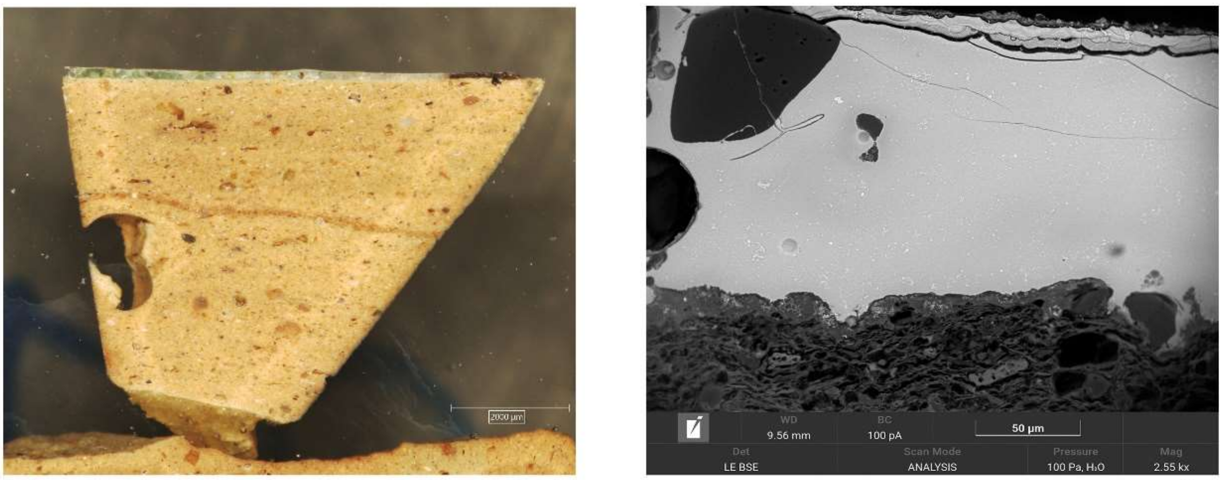

(a) (b)

Figure 7. Image collected on polished resin block by optical microscopy (**a**) and backscattered electron (BSE) image of the homogeneous white glaze of sample 50 (**b**) with underdeveloped ceramic/body–glaze interface.

The micro-structural analysis evidenced that glazes are rather homogenous; some isolated bubbles appear, slightly weathered on the surface, with some cracks (perpendicular or parallel to the surface) and with few unmelted quartz grains. Thickness varies between 90 and 160 μm. As already mentioned in the previous section, the ceramic matrix is enriched in CaO. Glaze thickness is variable, but glazes from the decorated side tend to be thicker. The ceramic/body glaze interface is rather thin, and newly formed acicular crystallites (3–9 μm long) can only be observed at high magnification. These observations indicate that decorations were applied on a biscuit-fired ceramic body [43], glazes were probably applied using frits [44,45], with the object undergoing cooling at a slow rate inside the kiln. PbO was the main flux employed, and alkalis contribution was below 5 wt% in all cases. The white glaze was obtained using SnO_2 [46,47], and it appears as acicular or sub-rounded micrometric inclusions with high contrast scattered homogenously within the glaze. Moreover, SnO_2 was also employed in green and black decorations but not in the honey glaze from the outer fragment side. The main colouring agents employed were MnO (black glaze) and CuO (green glaze). Conversely, in the outer glaze, considering the elevated concentration of Al_2O_3 and the lack of SnO_2, some clay was probably added to the glaze mixture. Broadly, the characteristics of the analysed sample match the technology applied in the Iberian Peninsula during the Islamic Middle Ages for this specific ceramic ware [1,40–42], and it is not possible to identify the origin. If compared with data obtained at Santarém [17], this piece shows a smaller amount of alkalis inside glazed decorations and similar ceramic paste characteristics in terms of CaO content. So, the only possible conclusion is that the piece was imported at the site, possibly from an unidentified location in southern Iberia, thus supporting the XRF results.

4.2. Raw Materials

4.2.1. Granulometry

Granulometric analysis evidenced that both raw materials show a high amount of sand, considering all sub-fractions. It is possible to observe that, based on the description of the ceramist, weak clay should be more enriched in inclusions. The observation of Figure 8 indicates that the strong clay is enriched in coarse, medium and fine sand. On the other hand, the weak clay is more enriched in very coarse sand, very fine sand and in clay containing silt. Thus, considering that every raw material is generally treated prior to its utilisation in order to increase the clay/temper ratio, results indicate that the weak clay is more enriched in finer grains. Nevertheless, by using only sieves, it is not possible to evaluate the amount of silt and clay separately, but the description of traditional ceramists regarding the weak clay seems adequate.

4.2.2. Powder X-Ray Diffraction Results of Clay Raw Materials—P-XRD

XRD results (Table 4) obtained by the analysis of strong and weak clays complemented granulometric observations. All samples are mainly composed of quartz, potassium-rich feldspars, plagioclase, rutile, illite/muscovite, kaolinite, smectite (strong clay) and vermiculite (weak clay). Thus, the identification of two different phyllosilicates mainly differentiates strong and weak clays. Moreover, as indicated by granulometric analyses, the applied sieving process also modified the tectosilicates+oxides/phyllosilicates ratio. In strong clay, phyllosilicate abundance gradually increases between untreated and the <63 μm fraction. In weak clay this effect is less strong. Besides, weak clay is generally more enriched in very fine sand particles and silt plus clay (Figure 8), agreeing with granulometric results.

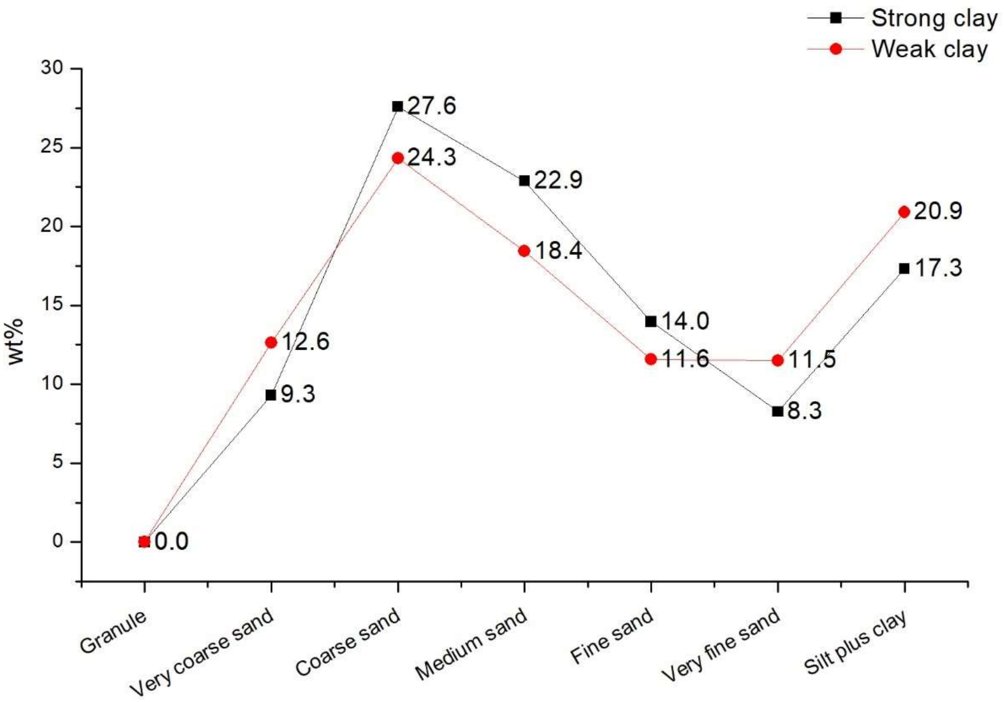

Figure 8. Granulometric analysis of strong and weak clays. Results expressed in percentage wt%.

Table 4. Semi-quantitative XRD results of strong and weak clays expressed in percentage (%). Q, quartz; H, hematite; Kf, potassium-rich feldspar, Pl, plagioclase; Ill/Mus, illite/muscovite; Kao, kaolinite; Rut, rutile; Smc, smectite; Ver, vermiculite.

Clay Type	Fraction	Q	Kf	Pl	Ill/Mus	Kao	Rut	Smc	Ver	Tectosilicates + Oxides	Phyllosilicates
Strong clay	Raw	36	27	2	27	3	1	4		66	34
	<500 µm	36	26	2	28	3	1	4		65	35
	<250 µm	29	24	4	32	4	1	6		58	42
	<125 µm	25	29	3	32	4	1	6		58	42
	<63 µm	25	22	3	39	4	1	6		48	52
Weak clay	Raw	28	28	8	25	3	1		7	62	38
	<500 µm	33	23	5	25	3	1		10	62	38
	<250 µm	32	23	5	29	3	1		8	61	39
	<125 µm	31	19	12	27	2	1		8	63	37
	<63 µm	26	26	8	30	3	1		6	61	39

4.2.3. X-Ray Fluorescence Results of Clay Raw Materials—XRF

As evidenced by XRF results, sediments show different chemical compositions, and data support granulometry and mineralogical observation. Aluminium and silicon oxides concentration varies coherently, and weak clay is enriched in SiO_2 and depleted in Al_2O_3 if compared to the strong clay. As evidenced by granulometry and XRD, this is the result of an enrichment of tectosilicates in the finer fraction of the sediment. Na_2O also tendentially increases in weak clay, suggesting that Na-rich plagioclase is also more represented in the finer fraction of the sediment.

Regarding trace elements, the weak clay is more enriched in Zr and depleted in Rb if compared to the strong clay. This tendency is coherent both in the raw (i.e., untreated), and in the finer fractions of the sediments. Zr is commonly abundant in sediments because of the resistance of zircon minerals to weathering, while Rb is normally hosted on potassium-rich mineralogical phases such as illite/muscovite. Moreover, the strong clay is generally more enriched in illite/muscovite if compared to the weak clay.

5. Comparing Ceramic and Sediments XRF Results

The chemical analysis comparison of ceramics and sediments (Figure 9) led to the identification of the raw material employed for the ceramic production at Serradinho archaeological site and the likely establishment of which samples were imported. First of all, it can be excluded that fabric 2 and fabric 3 were produced using either the weak or the strong clay. This is because, in any case, the chemical composition of samples does not match that of the sediments, specifically in reference to major oxides. The Fe_2O_3 concentration of fabric 2 samples is too low, and the sieving experiment performed evidenced that Fe_2O_3 is never lower than 5.51 wt% in sediments. In the case of fabric 3, none of the sediment showed a CaO concentration higher than 0.3 wt%. Thus, fabric 3 sample, does not match the chemical composition of both weak and strong clay or that of the Santarém area [17]. Regarding fabric 1, both sediments show a similar concentration of aluminium and silicon oxides. However, the original ratio of these two oxides in sediments could be voluntary and selectively altered by ancient ceramists modifying the original ratios with the addition of sand. This process was very common in ceramic production in every historical period, specifically to mitigate ceramic volume loss during the firing process [1,17,23,36,48]. Thus, the SiO_2/Al_2O_3 ratio cannot be employed for the direct comparison of sediments and ceramics in this case. The MgO vs. Na_2O binary plot evidences that fabric 1 samples, strong and weak clays, have a similar MgO concentration. Nevertheless, the weak clay is enriched in Na_2O, and, in any case, it cannot match fabric 1 samples' chemical composition, neither considering the raw nor the <63 µm sediment sample. This observation is coherent with the results obtained by sediment analyses in the previous sections (i.e., granulometry and mineralogy). Trace elements analysis confirms this observation. The binary plot Rb vs. Zr evidences how the trace elements concentration of the weak clay does not match that of fabric 1 ceramics. Rb is generally hosted by potassium-rich mineralogical phases such as potassium rich feldspars and illite/muscovite. In this case, illite/muscovite is particularly characteristic in strong clay if compared to the weak clay (Table 4), suggesting that strong clay was employed in ceramic production. Moreover, the Zr vs. Y binary plot indicates that strong clay and fabric 1 ceramic samples included the same zircon mineral. Yttrium generally substitutes Zr in the crystalline structure of the zircon mineral. As evidenced by different studies, the Zr/Y ratio is diagnostic to identify different zircon mineral populations which originally developed and crystallized in the same geochemical conditions [16,49,50]. Thus, it is possible to conclude that fabric 1 ceramic samples were produced using the strong clay raw material.

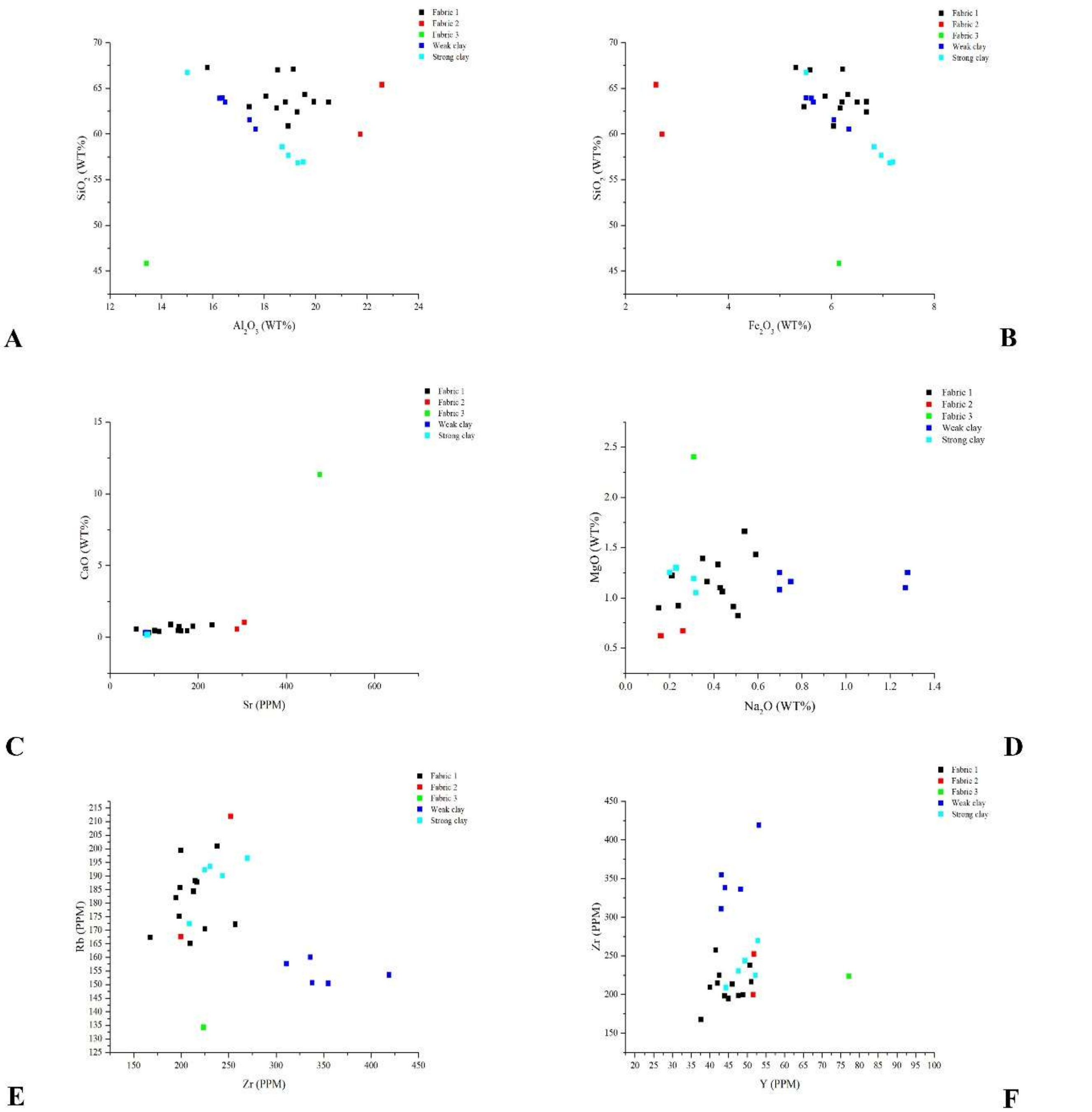

Figure 9. Binary plots of ceramic and sediment samples. (**A**) SiO_2 vs. Al_2O_3; (**B**) SiO_2 vs. Fe_2O_3; (**C**) CaO vs. Sr; (**D**) MgO vs. Na_2O; (**E**) Rb vs. Zr; (**F**) Zr vs. Y.

6. Conclusions

Archaeometric analyses of the archaeological ceramics recovered at the Serradinho archaeological site suggested that fabric 1 samples were produced using a locally available raw material. This includes common ware samples, normally employed for daily life activities. Considering archaeological ceramic relative chronology, the same raw material has been exploited over time. This indicates that the Middle Ages rural settlement of Serradinho was relatively independent from major pottery production centres. Nevertheless, it seems that few samples were not locally produced, such as red-painted and single-glaze decorated ceramics. In the first case, red-painted ceramics can be associated with the production identified at Santarém. Thus, it can be assumed that these artefacts were imported. This is plausible, considering that geographical proximity of Muge and

Santarém. In the second case, unfortunately, it is not possible to establish or even suggest a possible provenance. In any case, the incompatibility of the raw material employed for the production of sample 50 with locally available raw materials in the area (i.e., including Muge and Santarém) clearly indicates that it was imported into the settlement. To conclude, a long-standing exploitation of strong clay quarries for the production of fabric 1 from Islamic times to current traditional ceramics led by Domingos Gomes da Silva is really extraordinary. This underlies the importance of "tradition" in the sense that it can never be forgotten because it is absolutely connected to our roots.

Supplementary Materials: The following supporting information can be downloaded at: https://www.mdpi.com/article/10.3390/ceramics8020031/s1, Table S1: Chemical composition of ceramic and raw material samples obtained by X-Ray fluorescence, major oxides expressed in weight percentage (wt%), loss on ignition (L.O.I.), and the instrument statistical error; Table S2: Chemical composition of ceramic and raw material samples obtained by X-Ray fluorescence, trace elements expressed in part per million (ppm), and the instrument statistical error.

Author Contributions: Conceptualisation, M.B., N.S. and J.M.; methodology, M.B., N.S. and J.M.; formal analysis, M.B.; investigation, N.S., J.M. and M.B.; data curation, M.B.; writing—original draft, M.B.; writing—review and editing, C.A.C., G.L., N.S., J.M. and M.B. All authors have read and agreed to the published version of the manuscript.

Funding: This manuscript has been developed in the framework of the explorative project "GC-CIGA Glaze Ceramic Introduction and Consumption in the Gharb al-Andalus", granted by the Portuguese FCT to the corresponding author. Project code: 2023.13937.PEX, DOI: https://doi.org/10.54499/2023.13937.PEX.

Institutional Review Board Statement: Not applicable.

Informed Consent Statement: Not applicable.

Data Availability Statement: The original contributions presented in this study are included in the article/Supplementary Material. Further inquiries can be directed to the corresponding author.

Acknowledgments: The research team wish to acknowledge the FCT (Fundação para a Ciência e a Tecnologia) for funding the Hercules Laboratory (UIDB/04449/2020 – UIPD/04449/2020).

Conflicts of Interest: Author Gonçalo Lopes was employed by the Town Hall of Montemor O-Novo. The remaining authors declare that the research was conducted in the absence of any commercial or financial relationships that could be construed as a potential conflict of interest.

References

1. Beltrame, M. CALIPH: Comprehensive Archaeological and Laboratory Investigation of Islamic Pottery in Portuguese History. Ph.D. Thesis, University of Evora, Evora, Portugal, 2022. Available online: https://dspace.uevora.pt/rdpc/handle/10174/31377 (accessed on 12 September 2024).
2. Alves, M.S. Ocupação humana e polarização de um espaço rural do Gharb al-Andalus: O Médio Tejo à luz da toponímia árabica. In *Arquipélago. História, 2a Série*; Universidade dos Açores: Azores, Portugal, 1997; Volume 2, pp. 353–385, ISSN 0871-7664. Available online: https://hdl.handle.net/10400.3/474 (accessed on 5 October 2024).
3. Molina, L. *Una Descripción Anónima de al-Andalus (Dikr bilad al-Andalus)*; Consejo Superior de Investigaciones Científicas/Instituto Miguel Asín: Madrid, Spain, 1983.
4. Carvalho, J.D.R. Santarém e a Reconquista: A Tomada da Cidade em. Master's Thesis, University of Lisbon, Lisbon, Portugal, 2022. Available online: https://repositorio.ulisboa.pt/handle/10451/51698 (accessed on 6 October 2024).
5. Alves, M.S. *Uma Paisagem Humanizada. O Médio Tejo nos Finais da Idade Média I*; Patrimonia Historica: Cascais, Portugal, 2000.
6. Viana, M. A evolução do povoamento em Santarém na Idade Média e a sua relação com a área periurbana. In *Terceiras Jornadas de História sobre Paisagens Rurais e Urbanas: Fontes, Metodologias, Problemáticas, 2005*; Gonçalves, I., Ed.; Centro de Estudos Históricos da Universidade Nova de Lisboa: Lisbon, Portugal, 2007; pp. 83–108.
7. Liberato, M. Novos dados sobre a paisagem urbana da Santarém medieval (séculos V-XII): A necrópole visigoda e islámica de Alporão. *Medievalista* **2012**, *11*, 1–23. [CrossRef]

8. Lopes, G. Materiais do povoado Islâmico do Serradinho (Muge, Salvaterra de Magos). In *Cira Arqueologia*; Roque, F., Ed.; Câmara Municipal de Vila Franca de Xira and Museu Municipal: Vila Franca de Xira, Portugal, 2015; Volume 4, pp. 171–186, ISSN 2183069X.
9. Alves, M.S. Fronteira, guerra e organização social do espaço: O Vale do Tejo, entre muçulmanos e cristãos (séculos IX-XIII). In *Muçulmanos e Cristãos entre o Tejo e o Douro (Sécs. VIII a XIII)*; Barroca, M.J., Fernandes, I.C.F., Eds.; Câmara Municipal de Palmela/Facultade de Letras da Universidade do Porto: Palmela, Portugal, 2005; pp. 43–52.
10. Lopes, G. A propriedade régia em Muge durante a Idade Média. In *Magos-Revista Cultural do Concelho de Salvaterra de Magos*; Esménio, H.M., Ed.; Câmara Municipal de Salvaterra de Magos: Salvaterra de Magos, Portugal, 2018; Volume 5, pp. 3–28; Legal Deposit 380652/14.
11. Pinto, C.M.G. Gestos, Memórias e Formas Materiais Legadas Pelo Barro: A Produção Olárica no Ribatejo na Coleção de Olaria Tradicional do Museu Nacional de Etnología. Master's Thesis, NOVA University Lisbon, Lisbon, Portugal, 2012. Available online: https://hdl.handle.net/10362/7754 (accessed on 15 October 2024).
12. Vasconcellos, J.L. *Ceramica Portuguesa. Serie II, Estudos e Documentos Inéditos*; Typographia Elzeviriana: Porto, Portugal, 1884.
13. Lepierre, C. *Estudo Chimico e Technologico Sobre a Ceramica Portugueza Moderna*; Imprensa Nacional: Lisbon, Portugal, 1899.
14. Santos Júnior, J.R. Olarias de Muge (notas etnográficas). In *Trabalhos da Sociedade Portuguesa de Antropologia e Etnologia*; Imprensa Portuguesa: Porto, Portugal, 1932; Volume 5 (III), pp. 217–230.
15. Cardoso, G.; Batalha, L. Mestre Domingos Gonçalves da Silva: Um oleiro tradicional de Muge, Salvaterra de Magos. *Al-Madam* **2020**, *23*, 40–47.
16. Beltrame, M.; Liberato, M.; Mirão, J.; Santos, H.; Barrulas, P.; Branco, F.; Gonçalves, L.; Candeias, A.; Schiavon, N. Islamic and post Islamic ceramics from the town of Santarém (Portugal): The continuity of ceramic technology in a transforming society. *J. Archaeol. Sci. Rep.* **2019**, *23*, 910–928. [CrossRef]
17. Beltrame, M.; Sitzia, F.; Arruda, A.M.; Barrulas, P.; Barata, F.T.; Mirão, J. The Islamic ceramic of the Santarém Alcaçova: Raw materials, technology, and trade. *Archaeometry* **2021**, *63*, 1157–1177. [CrossRef]
18. Cunha, P.P. Cenozoic basins of Western Iberia: Mondego, lower Tejo and Alvalade basins. In *The Geology of Iberia: A Geodynamic Approach, Regional Geology Reviews*; Quesada, C., Oliveira, J.T., Eds.; Springer International Publishing: Cham, Switzerland, 2019; Volume 4: Cenozoic Basins, pp. 105–130. [CrossRef]
19. Cunha, P.P.; Martins, A.A.; Daveau, S.; Friend, P.F. Tectonic control of the Tejo river fluvial incision during the late Cenozoic, in Ródão-central Portugal (Atlantic Iberian border). *Geomorphology* **2005**, *64*, 271–298. [CrossRef]
20. Pais, J. The neogene of the lower Tagus basin (Portugal). *Revista Esp. Paleont.* **2004**, *19*, 229–242. [CrossRef]
21. Zbyszewski, G. Carta Geológica de Portugal na Escala de 1: Map 31-A Santarém Explicative Notes. Serviços Geológicos de Portugal: Lisbon, Portugal, 1952. Available online: https://geoportal.lneg.pt/download/maps/50k/news/31-A.pdf (accessed on 18 September 2024).
22. Zbyszewski, G.; Da Veiga, O. Carta Geológica de Portugal na Escala de 1: Map 31-C Coruche Explicative Notes; Serviços Geológicos de Portugal, Lisbon, Portugal. Available online: https://geoportal.lneg.pt/download/maps/50k/news/31-C.pdf (accessed on 23 September 2024).
23. Beltrame, M.; Sitzia, F.; Liberato, M.; Santos, H.; Themudo, F.; Columbu, S.; Mirão, J. Comparative pottery technology between the Middle Ages and Modern times (Santarém, Portugal). *Archaeol. Anthropol. Sci.* **2020**, *12*, 1–31. [CrossRef]
24. Quinn, P.S. *Ceramic Petrography: The Interpretation of Archaeological Pottery & Related Artefacts in Thin Section*, 1st ed.; Archaeopress: Oxford, UK, 2013; ISBN 978-1-905739-59-2.
25. Adams, A.E.; MacKenzie, W.S.; Guilford, C. *Atlas of Sedimentary Rocks Under the Microscope*, 1st ed.; Longman Group: London, UK, 1984; ISBN 0-582-02701-2.
26. Camara, C.; Gonçalves, M.J.; Mirão, J.A.; Gómez, S.M.; Beltrame, M. Morpho-functional, decorative and petrographic study of glazed/unglazed Islamic ceramics from the cities of Évora, Mértola and Silves. *Estud. Quaternário/Quat. Stud.* **2023**, *23*, 29–46. [CrossRef]
27. Hubbard, C.R.; Evans, E.H.; Smith, D.K. The reference intensity ratio, I/I c, for computer simulated powder patterns. *J. Appl. Cryst.* **1976**, *9*, 169–174. [CrossRef]
28. Camara, C.A.; Gonçalves, M.J.; Mirão, J.A.; Gómez, S.M.; Beltrame, M. High-lead glazed ceramic production in Western Iberia (Gharb al-Andalus) between the 10th and mid-13th centuries. An approach from the city of Évora (Portugal). *Ceramics* **2023**, *6*, 2213–2242. [CrossRef]
29. Schiavon, N.; Soria, V.; Arruda, A.M.; Beltrame, M.; Mirão, J. "Losanga" decorated imitations of italic late republican black gloss tableware from South-Western Iberia: A multi-analytical/microchemical characterization. *Microchem. J.* **2016**, *124*, 712–718. [CrossRef]
30. Duminuco, P.; Messiga, B.; Riccardi, M.P. Firing process of natural clays. Some microtextures and related phase compositions. *Thermochim. Acta* **1998**, *321*, 185–190. [CrossRef]
31. Riccardi, M.P.; Messiga, B.; Duminuco, P. An approach to the dynamics of clay firing. *Appl. Clay Sci.* **1999**, *15*, 393–409. [CrossRef]

32. Cultrone, G.; Rodriguez-Navarro, C.; Sebastian, E.; Cazalla, O.; De La Torre, M.J. Carbonate and silicate phase reactions during ceramic firing. *Eur. J. Mineral.* **2001**, *13*, 621–634. [CrossRef]
33. Trindade, M.J.; Dias, M.I.; Coroado, J.; Rocha, F. Mineralogical transformation of calcareous rich clays with firing: A comparative study between calcite and dolomite rich clays from Algarve, Portugal. *Appl. Clay Sci.* **2009**, *42*, 345–355. [CrossRef]
34. El Ouahabi, M.; Daoudi, L.; Hatert, F.; Fagel, N. Modified mineral phases during clay ceramic firing. *Clays Clay Miner.* **2015**, *63*, 404–413. [CrossRef]
35. Heimann, R.B.; Maggetti, M. The struggle between thermodynamics and kinetics: Phase evolution of ancient and historical ceramics. *Eur. Mineral. Union Notes Mineral.* **2019**, *20*, 233–281. [CrossRef]
36. Molera, J.; García-Vallés, M.; Pradell, T.; Vendrell-Saz, M. Hispano-Moresque pottery production of the fourteenth-century workshop of Testar del Molí (Paterna, Spain). *Archaeometry* **1996**, *38*, 67–80. [CrossRef]
37. Tite, M.S.; Freestone, I.; Mason, R.; Molera, J.; Vendrell-Saz, M.; Wood, N. Lead glazes in antiquity. Methods of production and reasons for use. *Archaeometry* **1998**, *40*, 241–260. [CrossRef]
38. Pradell, T.; Molera, J. Ceramic technology. How to characterize ceramic glazes. *Archaeol. Anthropol. Sci.* **2020**, *12*, 1–28. [CrossRef]
39. Nodari, L.; Marcuz, E.; Maritan, L.; Mazzoli, C.; Russo, U. Hematite nucleation and growth in the firing of carbonate-rich clay for pottery production. *J. Eur. Ceram. Soc.* **2007**, *27*, 4665–4673. [CrossRef]
40. Peréz-Arantegui, J.; Uruñuela, M.I.; Castillo, J.R. Roman glazed ceramics in the Western Mediterranean: Chemical characterization by inductively coupled plasma atomic emission spectrometry of ceramic bodies. *J. Archaeol. Sci.* **1996**, *23*, 903–914. [CrossRef]
41. Déléry, C. Using cuerda seca ceramics as a historical source to evaluate trade and cultural relations between Christian ruled lands and Al-Andalus, from the tenth to thirteenth centuries. *Al-Masāq* **2009**, *21*, 31–58. [CrossRef]
42. Chapoulie, R.; Déléry, C.; Daniel, F.; Vendrell-Saz, M. Cuerda seca ceramics from Al-Andalus, Islamic Spain and Portugal (10th-12th centuries AD): Investigation with SEM-EDX and cathodoluminescence. *Archaeometry* **2005**, *47*, 519–534. [CrossRef]
43. Molera, J.; Pradell, T.; Salvadó, N.; Vendrell-Saz, M. Interactions between clay bodies and lead glazes. *J. Am. Ceram. Soc.* **2001**, *84*, 1120–1128. [CrossRef]
44. Molera, J.; Pradell, T.; Salvadó, N.; Vendrell, M. Lead frits in Islamic and Hispano-moresque glazed productions. In *From Mine to Microscope: Advances in the Study of Ancient Technology*, 1st ed.; Shortland, A.J., Freestone, I.C., Rehren, T., Eds.; Oxbow Books: Oxford, UK, 2007; pp. 1–10, ISBN 978-184217-259-9.
45. Salinas, E.; Pradell, T.; Molera, J. Glaze production at early Islamic workshop in al-Andalus. *Archaeol. Anthropol. Sci.* **2018**, *11*, 2201–2213. [CrossRef]
46. Vendrell-Saz, M.; Molera, J.; Tite, M.S. Optical Properties of Tin-Opacified Glazes. *Archaeometry* **2000**, *42*, 325–340. [CrossRef]
47. Vendrell-Saz, M.; Molera, J.; Roqué, J.; Peréz-Arantegui, J. Islamic and Hispano-Moresque (múdejar) lead glazes in Spain: A technical approach. *Geol. Soc.* **2006**, *257*, 163–173. [CrossRef]
48. Molera, J.; Pradell, T.; Merino, L.; García-Vallés, M.; García-Orellana, J.; Salvadó, N.; Vendrell-Saz, M. La tecnología de la cerámica Islámica y Mudéjar. *Caesaraugusta* **1997**, *73*, 15–41.
49. Murad, E. Yttrium and zirconium as geochemical guide elements in soil and stream sediment sequences. *J. Soil Sci.* **1978**, *29*, 219–223. [CrossRef]
50. Fedo, C.M.; Sircombe, K.N.; Rainbird, R.H. Detrital zircon analysis of the sedimentary record. *Rev. Mineral. Geochem.* **2003**, *53*, 277–303. [CrossRef]